14th International Beam Instrumentation Conference,Liverpool, UK JACoW Publishing
ISBN: 978-3-95450-262-2 ISSN: 2673-5350 doi: 10.18429/JACoW-IBIC2025-TUPCO02

COMMISSIONING OF A LASER WIRE PROFILE MONITOR PROTOTYPE AT CSNS*

B. Zhang, C. Chen, S. Yan, Z. Xu, R. Liu, J. Wei, P. Zhu, R. Yang†, X. Li, S. Wang
Institute of High Energy Physics, Beijing, China
also at China Spallation Neutron Source, Dongguan, China
P. Ding, School of Nuclear Science and Technology, Lanzhou University, Lanzhou, China

Abstract

China Spallation Neutron Source (CSNS) accelerator complex will employ a new superconducting accelerating section to achieve high beam power. To protect the superconducting cavity from contamination, the CSNS superconducting linac section will adopt laser stripping technology for transverse distribution measurements of the negative hydrogen beam at nine stations. Recently, a laser wire (LW) prototype was installed to measure the profile of the 80 MeV H^- beam in a non-invasive manner. This paper presents the design and commissioning of this LW prototype.

INTRODUCTION

The China Spallation Neutron Source (CSNS) linear accelerator (linac) will be upgraded with a superconducting section, boosting the beam energy from 80 MeV to 300 MeV and increasing the Rapid Cycling Synchrotron (RCS) beam power from 100 kW to 500 kW [1, 2]. To prevent contamination of the superconducting cavities from broken physical wires, a non-destructive diagnostic method was developed [3, 4]. This method uses a 1064 nm laser to ionize H^- ions (binding energy 0.75 eV), with the resulting electrons, proportional to the local ion density, collected to reconstruct the beam profile as the laser scans the beam [5–9]. A laser wire profile measurement device was installed at CSNS in 2024 to test this approach, and this paper details its design and commissioning results.

LASER WIRE SYSTEM

Figure 1 provides a schematic overview of the entire laser wire system. The CSNS linac comprises a radio-frequency quadrupole (RFQ) that accelerates the negative hydrogen beam to 3 MeV and four drift tube linacs (DTLs) that further accelerate the beam to 80 MeV. For the upgrade of the emittance monitor [10, 11], the laser wire station is allocated in the linac transport beam line (about 150 m downstream of the DTL), where the beam energy is 80 MeV. The time structure of the pulsed beam in the linac, shaped by an RF chopper cavity for RCS injection, is depicted in Fig. 2. The beam pulse consists of 324 MHz micro-bunches, 550 ns intermediate bunches, and a 750 µs (max.) macro-pulse with a repetition rate of 25 Hz. A high-power Q-switched Nd:YAG laser, operating at 1064 nm, serves as the light source for efficient photo-detachment. This laser has a full width at half maximum (FWHM) of approximately 10 ns and a repetition rate of 1-10 Hz. By synchronizing the timing between the beam and the laser, the laser can precisely interact with a specific intermediate bunch, detaching approximately six micro-bunches per laser pulse. The demonstrated synchronization timing jitter is about 1 ns.

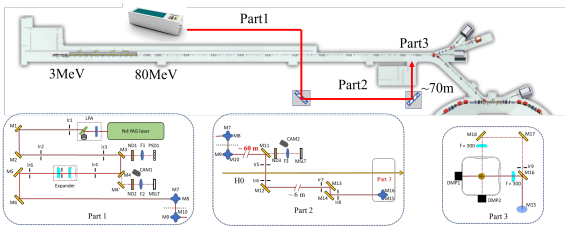

Figure 1: Outline of the laser wire system installed in the CSNS linac.

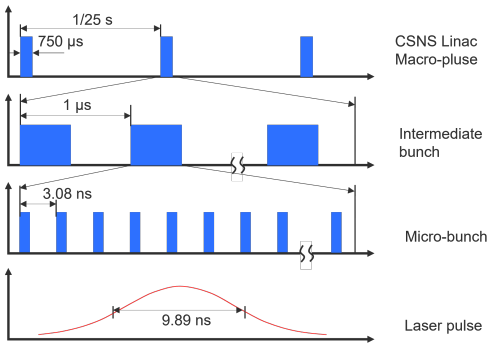

Figure 2: Time structure of the pulses beam in the CSNS linac.

The number of stripped electrons is related to the laser energy and is assessed by

$$-\mathrm{d}n = \sigma(E_{\mathrm{cm}}) \times \Phi(x, y, z, t) \times n(t)dt, \qquad (1)$$

where $n(t)$ is the number of negative hydrogen beam in an elementary volume element, $\sigma(E_{\mathrm{cm}})$ is the photodetachment cross-section [12], and Φ is the photo flux. For an averaged H^- beam current of 10 mA and a laser pulse energy of more than 100 mJ, there are approximately $10^4 - 10^7$ electrons are detached. These photodetached electrons are deflected by a C-shaped magnet and strike the Faraday cup in the vertical

* Work supported by National Natural Science Foundation of China (No. 12305166), the Natural Science Foundation of Guangdong Province, China (No. 2024A1515010016) and National Key R&D Program of China under Contracts No. 2023YFE0105700.
† yangrenjun@ihep.ac.cn

ISBN: 978-3-95450-262-2 ISSN: 2673-5350 doi: 10.18429/JACoW-IBIC2025-TUPCO02

direction, while the main negative beam remains largely unaffected as shown in Fig. 3. The Faraday cup is connected to a short 50 Ω transmission line, followed by a transition to an SMA-type feedthrough. A preamplifier with a gain of 20 dB and a bandwidth extending to 2 GHz is installed near the station in the tunnel to amplify the signal from the feedthrough and reduce the impact of thermal noise introduced during transmission on the original signal. Then the amplified electrical signal is transmitted to an analog-to-digital converter (ADC) for data analysis and profile measurement.

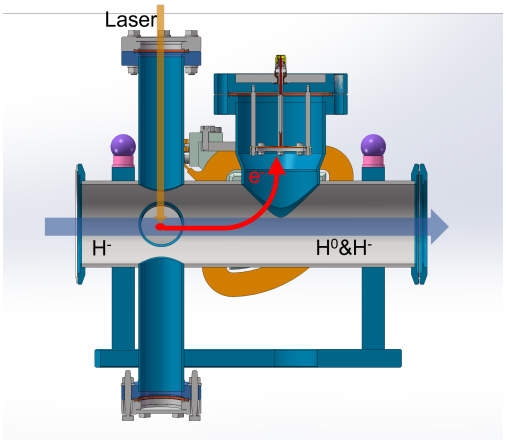

Figure 3: A schematic diagram of the laser wire principle.

COMMISSIONING OF THE LASER WIRE PROTOTYPE

A stainless steel honeycomb structure with a nickel coating, 6 mm thick and featuring 3.2 mm hexagonal holes, is positioned downstream of a magnet as an RF shield to suppress induced image currents on the anodes. Its electromagnetic compatibility was evaluated using a Goubau Line, which transmitted beam-like electromagnetic waves with a 2 kV, 2 ns pulse at a repetition rate of 25 Hz. The shield demonstrated a shielding effectiveness of −52.6 dB, as shown in Fig. 4. However, during operation, some electrons impacted the grid despite the structure providing sufficient clearance.

Following the installation of the laser wire system last summer, we evaluated the noise characteristics of the Faraday cup, as shown in Fig. 5. Initially, in the absence of a beam, significant noise signals were observed, which increased with higher input current to the deflection magnets. By averaging multiple signals, the noise was eliminated, confirming that it originated from the ripple of the magnet power supply. Subsequently, the power supply was replaced with a low-ripple version, reducing the noise to a level of ±7 mV. After the accelerator began supplying the beam, we initially investigated the impact of varying deflection magnet currents on the collection efficiency of stripped electrons. The deflection magnet redirects electrons produced by laser stripping, enabling them to reach the Faraday cup and generate an electron signal. At the laser wire monitor position, the beam exhibits a horizontal and vertical momentum spread

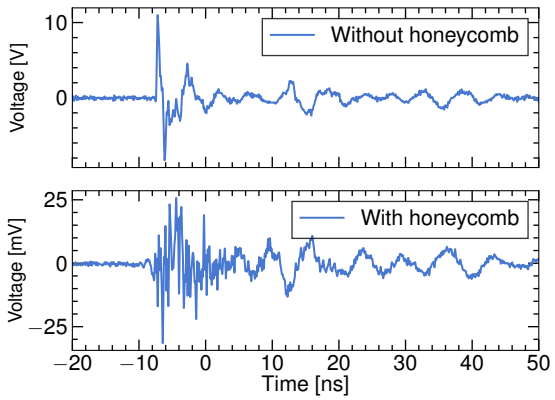

Figure 4: The shielding effectiveness of honeycomb.

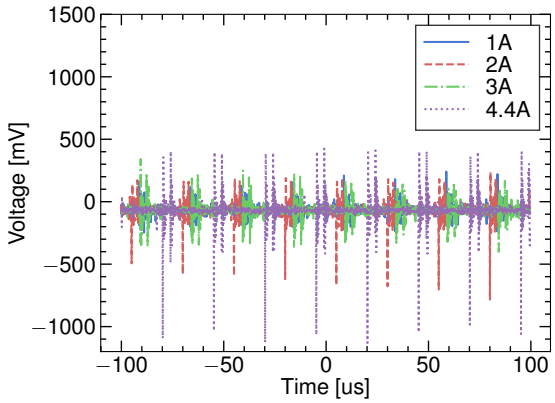

Figure 5: Noise from Faraday cup caused by magnet power supply.

of approximately 0.1 mrad, resulting in minimal dispersion of the stripped electrons. A large-aperture Faraday cup is designed to collect all stripped electrons. In principle, while varying the magnet current alters the electron trajectories, within a certain range, the Faraday cup should collect 100 % of the electrons. However, the relationship between the number of collected stripped particles and the magnet current, as shown in Fig. 6, reveals a serrated structure rather than the expected trapezoidal profile. This is primarily due to the honeycomb structure used for electromagnetic shielding, which partially obstructs the electrons produced by laser stripping. Different magnetic induction intensities lead to variations in electron trajectories, resulting in differing obstruction ratios. A simulation using the Particle Tracking module in CST Studio Suite validated these findings. To obtain a beam profile closer to the true profile, a magnet current of 5.84 A, which maximizes the number of stripped electrons, was selected as the optimal parameter for the profile scan.

An incident laser energy of 100 mJ is sufficient to produce a stripped electron signal of 200 mV, achieving an excellent signal-to-noise ratio. Further increasing the laser energy does not significantly enhance the stripped electron signal. Due to potential variations in the beam position, the focusing mirror must be adjusted before each profile scan to ensure that the laser focus aligns with the beam center for better

ISBN: 978-3-95450-262-2 ISSN: 2673-5350 doi: 10.18429/JACoW-IBIC2025-TUPCO02

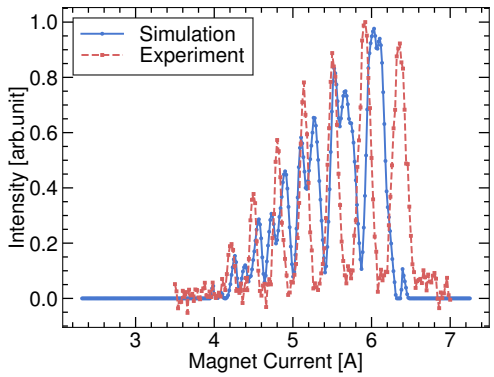

Figure 6: Detected electron pulse integration at different deflection magnet current.

spatial resolution. Under this aligned condition, the collected stripped electron signal is minimized.

MEASUREMENT RESULT

We varied the laser pulse energy at the vacuum window entrance and measured the electron pulse integration using Faraday cup (FC) and photodiode (PD) outputs, as shown in Fig. 7. Error bars represent the standard deviation of 10 pulses. The PD output shows the expected linear dependence on laser energy. The FC output initially increases linearly with laser energy but plateaus beyond 100 mJ, where stripping efficiency reaches 100 % in the laser-beam interaction region. Further energy increases mainly affect electrons at the pulse edges, contributing little to the total stripped particles, consistent with simulation results. This explains why the FC signal is not normalized to the PD signal. Above 300 mJ, discrepancies between simulation and experiment are due to stray light effects.

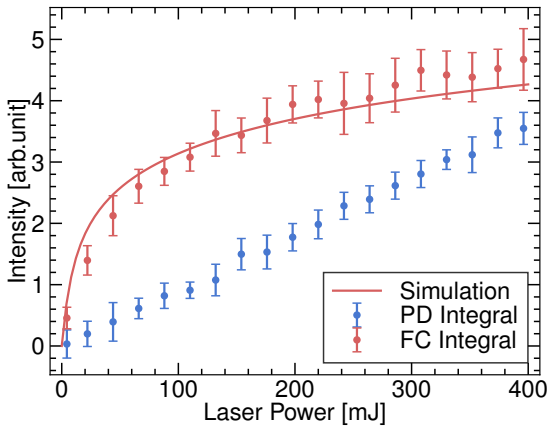

Figure 7: Detected electron pulse integration from FC and PD versus laser pulse energy.

The ion beam profile was measured by scanning a laser beam across it and recording the integrated signal as a function of laser position. A 1 Hz trigger, synchronized with the ion beam, ensures consistent timing among the laser, beam,

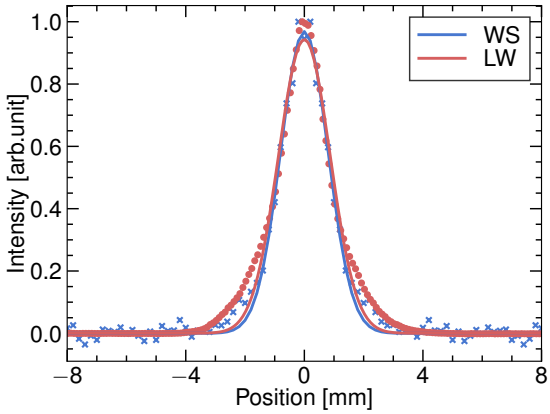

Figure 8: Overlay of minimum profiles of laser wire and wire scanner.

and detector signal through an acquisition card. To mitigate bias from the acquisition board, the average signal over the final 80 ns of data is used as the background noise level and subtracted from the profile scan. By plotting and fitting the correlation between the laser wire scanning position and the integrated value of the acquired raw signal, the transverse profile of the H^- beam can be reconstructed.

To validate the accuracy of the laser wire profile measurement system, the honey-comb structure has been removed. By adjusting the quadrupole current upstream of the laser wire, the beam is focused at the LW and a wire scanner located about 1.5 m upstream. The beam sizes at the waist are then measured by the two instruments and plotted in Fig. 8. The discrepancy between the two measurements is about 8 %. This discrepancy might be explained by the inner-pulse beam position displacement.

CONCLUSION

A laser wire prototype has been successfully commissioned at CSNS. After transmission over 80 m to the laser wire station, the system achieved a beam quality factor of 4 and a transmission efficiency of 83.8 %. For a deflection magnet current to 5.84 A and the input laser power to 100 mJ, the rms beam size obtained by the laser-wire monitor is about 8% lower than the wire-scanner. To reduce electron obstruction, a new interaction chamber without the honeycomb structure has been placed on beamline. Additionally, a beam splitter combined with an optical delay line will be implemented to sequentially direct the laser beam into the vacuum window along the horizontal and vertical directions, enabling simultaneous measurement of both the horizontal and vertical beam profiles.

ISBN: 978-3-95450-262-2 ISSN: 2673-5350 doi: 10.18429/JACoW-IBIC2025-TUPCO02

REFERENCES

[1] S. Fu and S. Wang, "Operation status and upgrade of CSNS", in *Proc. IPAC'19*, Melbourne, Australia, May 2019, pp. 23–27. doi:10.18429/JACoW-IPAC2019-MOZPLM1

[2] J. Wei *et al.*, "China Spallation Neutron Source: design, R&D, and outlook", *Nucl. Instrum. Methods Phys. Res. A*, vol. 600, no. 1, pp. 10–13, 2009. doi:10.1016/j.nima.2008.11.017

[3] Y. Liu, C. Long, C. Peters, and A. Aleksandrov, "Measurement of ion beam profiles in a superconducting linac with a laser wire", *Appl. Opt.*, vol. 49, no. 35, pp. 6816–6823, 2010. doi:10.1364/AO.49.006816

[4] Y. Liu *et al.*, "Laser wire beam profile monitor in the spallation neutron source (SNS) superconducting linac", *Nucl. Instrum. Methods Phys. Res. A*, vol. 612, no. 2, pp. 241–253, 2010. doi:10.1016/j.nima.2009.10.061

[5] T. Hofmann, G. E. Boorman, A. Bosco, S. M. Gibson, and F. Roncarolo, "A low-power laserwire profile monitor for H^- beams: design and experimental results", *Nucl. Instrum. Methods Phys. Res. A*, vol. 903, pp. 140–146, 2018. doi:10.1016/j.nima.2018.06.035

[6] Y. Liu, C. Long, C. Huang, R. Dickson, and A. Aleksandrov, "Simultaneous ion beam profile scan using a single laser source", *Phys. Rev. Spec. Top. Accel. Beams*, vol. 16, no. 1, p. 012801, 2013. doi:10.1103/PhysRevSTAB.16.012801

[7] S. T. Boogert *et al.*, "Micron-scale laser-wire scanner for the KEK accelerator test facility extraction line", *Phys. Rev. Spec. Top. Accel. Beams*, vol. 13, no. 12, p. 122801, 2010. doi:10.1103/PhysRevSTAB.13.122801

[8] R. Connolly *et al.*, "A laser-wire beam-energy and beam-profile monitor at the BNL LINAC", in *Proc. NAPAC'11*, New York, NY, USA, Mar.–Apr. 2011, paper MOP194, pp. 456–458.

[9] Y. Liu, C. Long, W. Grice, W. Blokland, and S. Assadi, "Laser wire beam profile monitor at SNS", in *Proc. EPAC'08*, vol. 8, Genoa, Italy, Jun. 2008, paper TUPC061, pp. 1197–1199.

[10] Y. Liu *et al.*, "Nonintrusive emittance measurement of 1 GeV H^- beam", *Nucl. Instrum. Methods Phys. Res. A*, vol. 675, pp. 97–102, 2012. doi:10.1016/j.nima.2012.02.009

[11] T. Hofmann *et al.*, "Experimental results of the laserwire emittance scanner for LINAC4 at CERN", *Nucl. Instrum. Methods Phys. Res. A*, vol. 830, pp. 526–531, 2016. doi:10.1016/j.nima.2016.02.018

[12] H. Takei, K. Tsutsumi, and S.-I. Meigo, "Low-power proton beam extraction by the bright continuous laser using the 3-MeV negative-hydrogen linac in japan proton accelerator research complex", *J. Nucl. Sci. Technol.*, vol. 58, no. 5, pp. 588–603, 2021. doi:10.1080/00223131.2020.1848654